AIAA SciTech Forum
January 3-7, 2022, San Diego, CA & Virtual
AIAA SCITECH 2022 Forum

10.2514/6.2022-0396

Anomalous Waves in Non-Ideal Detonation Dynamics

Katherine R. Pielemeier * and Joseph M. Powers†
University of Notre Dame, Notre Dame, Indiana, 46556-5637

A study of inviscid reactive flows in BZT (Bethe-Zel'dovich-Thompson) gases with anomalous waves is introduced. BZT gases are non-ideal gases that may present anomalous waves such as isentropic compressions, discontinuous rarefactions, and split or composite waves comprised of connected continuous and discontinuous waves. Exact solutions for discontinuous shocks and continuous isentropic fans in a van der Waals gas are computed for inert flows, and some features of anomalous waves are discussed. Thermodynamics predicts that a piston moving into an ideal gas at rest may induce a discontinuous compression shock. When the gas reacts, the resulting structure of the reaction zone is well known for an ideal gas. A BZT gas in the anomalous region of state space will instead form a continuous isentropic compression fan or split compression wave. Modeling the flow with a non-ideal gas equation of state affects the sound speed, wave speed, and reaction rate. The effect of the non-ideal van der Waals parameters on the reaction rate and wave speed will be shown.

I. Nomenclature

$\mathcal{A}$	=	reaction rate multiplier
a, b	=	van der Waals parameters
c	=	sound speed
c_v	=	specific heat at constant volume
D	=	shock speed
e	=	specific internal energy
f	=	flux function
$\hat{f}$	=	numerical flux function
$\mathcal{G}$	=	fundamental derivative
p	=	pressure
p_c	=	critical pressure
p_o	=	reference pressure
q	=	heat release per unit mass
R	=	particular gas constant
r	=	reaction rate
s	=	specific entropy
s_o	=	reference entropy
T	=	temperature
T_c	=	critical temperature
T_o	=	reference temperature
t	=	time
Δt	=	time step size
u	=	x-velocity
v	=	specific volume
v_o	=	reference specific volume
x	=	Cartesian spatial coordinate
Δx	=	spatial step size

*Ph.D. Candidate, Department of Aerospace and Mechanical Engineering, University of Notre Dame, Notre Dame, Indiana 46556-5637, kpieleme@nd.edu, AIAA Student Member.

†Professor, Department of Aerospace and Mechanical Engineering, University of Notre Dame, Notre Dame, Indiana 46556-5637, powers@nd.edu, AIAA Associate Fellow.

α = flux splitting weight
δ = c_v/R
$\mathcal{E}$ = activation energy
γ = ratio of specific heats for an ideal gas
λ = reaction progress variable
ρ = density
ω = WENO scheme weights

II. Introduction

Modeling of inviscid reactive flows in non-ideal gases with anomalous waves has yet to see a thorough investigation. Reactions behind classical discontinuous compression shocks are well understood [1]. We consider non-ideal gas flows where anomalous waves, namely discontinuous rarefactions, continuous compressions, and split or composite waves, are present. The first studies on the existence and theory of anomalous waves were done by Bethe [2], Zel'dovich [3], and later Thompson [4]. It was established that given a particular set of conditions, anomalous waves may exist in single-phase gases in the neighborhood of the critical point [3]. In this anomalous region, sometimes called the BZT (Bethe-Zel'dovich-Thompson) region, the isentropes in the pressure-specific volume plane are non-convex, and discontinuous rarefaction shocks and continuous compression fans are admissible. It is straightforward to prove that these anomalous waves satisfy the second law of thermodynamics.

Since Bethe, Zel'dovich, and Thompson's original discussions of anomalous waves, a number of fluid classes have been determined to meet the criteria to exhibit anomalous waves as a single phase gas. These include hydrocarbons and fluorocarbons ([5], [6], [7]), and siloxanes ([8], [9], [10]). Further investigation of these candidate BZT fluids has been conducted by Colonna and Guardone [11] and Harinck *et al.* [12]. These studies discerned that a key parameter is the molecular complexity of the fluid, primarily the number of active degrees of freedom of the molecule.

Many studies have sought to better understand the anomalous wave structures possible in BZT fluids. Cramer and Sen [13] investigated shock formation in an arbitrary inviscid van der Waals gas, demonstrating the formation of composite waves resulting from changes in convexity of the isentrops. Cramer and Crickenberger [14] studied the structure of expansion shocks, confirming that when an isentrope changes convexity, the sound speed no longer changes monotonically. Cramer [15] also gave detailed descriptions of the conditions under which shock splitting occurs. Like isentropes, shock adiabats may also exhibit changes in convexity, and as a result Rayleigh lines may intersect the shock adiabat at more than two points. The Rankine-Hugoniot jump conditions have more than two solutions, but only between neighboring roots are these solutions valid. Cramer concludes that split shock structures, where discontinuities and fans travel as one, evolve dynamically from inadmissable initial configurations. More recently, Guardone, *et al.* [16] and Zamfirescu, *et al.* [17] have investigated the maximum intensity and admissibility region for rarefaction shock waves. It was determined that this region is slightly larger than the BZT region.

No previous study has been identified that considers anomalous wave dynamics in detonating BZT gases. Here, we will consider detonations in a model fluid with the behavior of BZT gases, and study the influence of non-ideal effects on detonation dynamics. We will begin with specification of the governing equations and constitutive realations. The van der Waals equation of state is chosen, and conditions for anomalous waves are introduced, including the fundamental derivative. Exact solutions for compression and rarefaction shocks and fans in inert van der Waals gases are presented, and key features are highlighted. A description is given of the numerical scheme. Finally, some effects of non-idealities on the reaction behind a compression shock are presented, and the difficulties in extending this study to reactions behind anomalous compression waves are discussed.

III. Governing Equations

The inviscid one-dimensional unsteady reactive Euler equations for a general equation of state with a one step irreversible reaction are given in conservative form.

$$\frac{\partial \rho}{\partial t} + \frac{\partial}{\partial x}(\rho u) = 0, \tag{1}$$

$$\frac{\partial}{\partial t}(\rho u) + \frac{\partial}{\partial x}(\rho u^2 + p) = 0, \tag{2}$$

$$\frac{\partial}{\partial t}\left(\rho\left(e + \frac{1}{2}u^2\right)\right) + \frac{\partial}{\partial x}\left(\rho u\left(e + \frac{1}{2}u^2 + \frac{p}{\rho}\right)\right) = 0, \tag{3}$$

$$\frac{\partial}{\partial t}(\rho\lambda) + \frac{\partial}{\partial x}(\rho u\lambda) = \rho r, \tag{4}$$

$$e = e(\rho, T, \lambda), \tag{5}$$

$$p = p(\rho, T, \lambda), \tag{6}$$

$$r(T, \lambda) = \mathcal{A}(1 - \lambda)\exp\left(\frac{\mathcal{E}}{RT}\right). \tag{7}$$

Independent variables are t and x, time and the Cartesian space coordinate respectively. Dependent variables are density ρ, particle velocity u, pressure p, specific internal energy e, reaction progress λ, and temperature T. Parameters are the particular gas constant R, the reaction rate constant $\mathcal{A}$, and the activation energy $\mathcal{E}$.

Equations (1-3) represent the conservation of mass, linear momentum, and energy. Equation (4) represents the species evolution, with an irreversible reaction A→B where the molecular mass and specific heats are identical for both species. The mass fractions are related to the reaction progress variable by $Y_A = 1 - \lambda$ and $Y_B = \lambda$; therefore, λ varies from 0 to 1. Equations (5) and (6) are general constitutive relations for the caloric and thermal equations of state respectively. Anomalous waves can be predicted by a non-ideal equation of state with regions where the fundamental derivative $\mathcal{G}$ is negative (see [4], [13], and [18]). For this work the van der Waals equation of state has been chosen, and the constitutive relations are now

$$e(\rho, T, \lambda) = c_v T - a\rho - \lambda q, \tag{8}$$

$$P(\rho, T, \lambda) = \frac{\rho RT}{1 - \rho b} - a\rho^2. \tag{9}$$

The van der Waals constants a and b are defined by $a = 27R^2T_c^2/64/p_c$ and $b = RT_c/8/P_c$, where T_c and p_c are the critical temperature and pressure respectively. Additional useful expressions include the sound speed

$$c^2 = \frac{RT}{(1 - b/v)^2}\left(1 + \frac{R}{c_v}\right) - \frac{2a}{v}, \tag{10}$$

where the specific volume v is related to the density by $v = 1/\rho$, and the specific entropy

$$\frac{s - s_o}{c_v} = \ln\left(\frac{T}{T_o}\right) + \frac{R}{c_v}\ln\left(\frac{v - b}{v_o - b}\right), \tag{11}$$

with specific heat at constant volume c_v and reference parameters s_o, T_o, and v_o.

Introduced formally by Thompson [4], the non-dimensional fundamental derivative of gasdynamics $\mathcal{G}$ is defined by:

$$\mathcal{G}(s, v) \equiv -\frac{\frac{v}{2}\left.\frac{\partial^2 p}{\partial v^2}\right|_s}{\left.\frac{\partial p}{\partial v}\right|_s} = \frac{v^3}{2c^2}\left.\frac{\partial^2 p}{\partial v^2}\right|_s. \tag{12}$$

Because $v^3/2c^2$ is always positive, the sign of $\mathcal{G}$ is determined by $(\partial^2 p/\partial v^2)_s$. The fundamental derivative gives a measure of the convexity of isentropes in the p-v plane. The sign of $\mathcal{G}$ determines the types of waves that may form: when $\mathcal{G} > 0$, only discontinuous compressions and continuous rarefactions will form, and when $\mathcal{G} < 0$, only anomalous waves will form. Using Eqs. (12, 9, 10, 11), we can write the fundamental derivative for a van der Waals gas as

$$\mathcal{G}(v, s) = \frac{v^3}{2c^2}\left(-\frac{6a}{v^4} + \frac{RT_o}{c_v}\left(\frac{R}{c_v} + 2\right)\frac{R + c_v}{(v - b)^3}\exp\left(\frac{s - s_o}{c_v}\right)\left(\frac{v - b}{v_o - b}\right)^{-R/c_v}\right). \tag{13}$$

The upper boundary on the region of state space where anomalous waves may occur is bounded by the curve $\mathcal{G} = 0$, below which $\mathcal{G} < 0$. This can be found by converting $\mathcal{G}(s, v)$ to $\mathcal{G}(p, v)$, setting the resulting function equal to zero, and solving for pressure as a function of specific volume. For a van der Waals gas the resulting function is

$$p(v) = \frac{6c_v a}{v^4} \frac{(v-b)^2}{(R+c_v)(R/c_v+2)} - \frac{a}{v^2}. \tag{14}$$

The region of negative fundamental derivative in the gas phase is typically found in the neighborhood of the critical point, and anomalous, or BZT, regions are often limited to a small area of state space.

IV. Anomalous Waves - Examples

Some examples of anomalous waves in an inert gas are given; exact solutions for isentropic waves in van der Waals gases have been found using an adaption of the ideal gas solution from von Mises [19] and Courant and Friedrichs [20]. Classically, the isentropic fan is a rarefaction and the discontinuous shock is a compression; however, the solutions admit isentropic compressions and discontinuous rarefaction shocks as well. The exact solutions for discontinuous shocks, either a rarefaction or compression, are straightforward with the required substitution of the van der Waals equation of state. In the steady frame traveling with a shock of speed D, the Rankine-Hugoniot jump conditions for a general equation of state can be written as

$$\rho_2 \hat{u}_2 = \rho_1 \hat{u}_1, \tag{15}$$

$$\rho_2 \hat{u}_2^2 + p_2 = \rho_1 \hat{u}_1^2 + p_1, \tag{16}$$

$$e_2 + \frac{1}{2}\hat{u_2^2} + \frac{p_2}{\rho_2} = e_1 + \frac{1}{2}\hat{u_1^2} + \frac{p_1}{\rho_1}, \tag{17}$$

$$\lambda_2 = \lambda_1, \tag{18}$$

$$e = e(\rho, p, \lambda). \tag{19}$$

The $\hat{u}$ indicates the velocity in the wave frame, and the velocity in the lab frame can be recovered with $\hat{u} = u - D$. Equations (15-19) form a system of five equations for the five unknowns: ρ_2, $\hat{u}_2$, p_2, e_2, and λ_2. Across a shock, the reaction progress does not change, and these equations hold for an inert system as well as with reaction. Additionally, these jump equations hold for both rarefaction and compression shocks. Figures (1) and (2) show exact solutions of a discontinuous compression shock and rarefaction shock respectively; arrows indicate the direction the wave travels, and accompanying arrows indicate the wave speed relative to the leading edge of the wave. The compression shock, traveling to the right, behaves as expected of a discontinuous shock, raising the density. The rarefaction shock, traveling to the right, decreases the density, but raises the sound speed, resulting in a discontinuous rarefaction that does not decay into a continuous rarefaction wave.

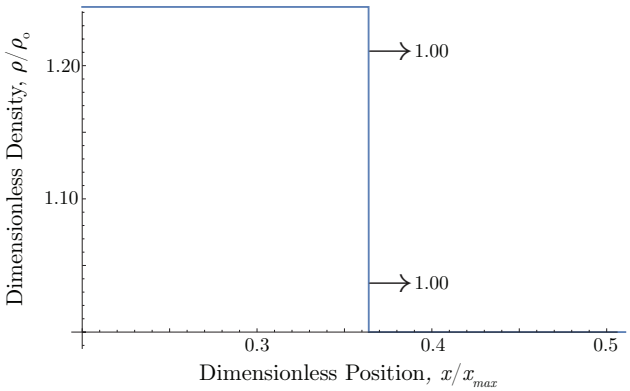

Fig. 1 Conventional compression shock, fundamental derivative $\mathcal{G} > 0$; arrows indicate the direction the wave travels, accompanying numbers indicate the wave speed, normalized by its maximum value on the wave. Density and sound speed increase across the shock.

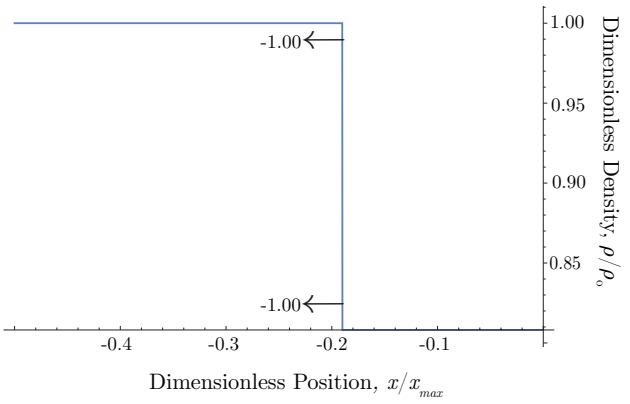

Fig. 2 Rarefaction shock, fundamental derivate $\mathcal{G} < 0$; arrows indicate the direction the wave travels, accompanying numbers indicate the wave speed, normalized by its maximum value on the wave. Sound speed increases across the shock, even though the density has decreased.

The isentropic solutions were computed using Riemann invariants for a centered simple wave, as described by Courant and Friedrichs [20] and von Mises [19]. Assuming isentropic flow, characteristic analysis can be used to arrive at the following equations:

$$u + \hat{l}(\rho) = 2r(\beta_r), \tag{20}$$

$$u - \hat{l}(\rho) = -2s(\alpha_s), \tag{21}$$

where $r(\beta_r)$ and $s(\alpha_s)$ are arbitrary functions, called Riemann invariants, and $\hat{l}(\rho)$ is defined by:

$$\hat{l}(\rho) = \int_{\rho'}^{\rho} \frac{c(\hat{\rho})}{\hat{\rho}} d\hat{\rho}. \tag{22}$$

If this integration is possible analytically, functions for $u(x)$ and $u(t)$ can be written. Using the characteristics

$$\frac{dx}{dt} = u \pm c(\rho), \tag{23}$$

and isentropic relations, a full solution for an isentropic wave, either a rarefaction or compression, can be found. However, for the van der Waals equation of state, the isentropic sound speed $c(\rho)$ is given by

$$c(\rho) = \sqrt{-2a\rho - \frac{\hat{c}(1 - R/c_v)(1/\rho - b)^{-R/c_v}}{\rho^2}}, \tag{24}$$

where $\hat{c}$ is a constant. Substituting Eq. (24) into (22), the integral cannot be computed analytically. An additional step is required, and using a numerical quadrature, a functional form of $u(\rho)$, containing an integral, can be constructed. If we set u to be the velocity of a piston, u_p, the characteristics can be written as:

$$\frac{dx}{dt} = u_p \pm c(\rho(u_p)), \tag{25}$$

where we can now find the density as a function of the piston velocity, and from there the sound speed. Isentropic relations for van der Waals are used to find the remaining flow variables. Solutions for both forward and backward facing, as well as compression and rarefaction, isentropic fans can be computed in this way.

We first have a rarefaction fan, traveling to the left, in Fig. 3, where density decreases continuously across the wave. This corresponds to a decrease in sound speed, as expected of classical wave behavior. In regions where the fundamental derivative is negative, rarefactions increase the sound speed, resulting in the discontinuous rarefactions as seen previously. Similarly, compressions are continuous fans rather than discontinuous shocks, as shown in the right moving wave in Fig. (4). Across such a continuous compression, the sound speed decreases, so the leading edge of the wave moves at a larger speed than the trailing edge, and the wave does not collapse to a discontinuity.

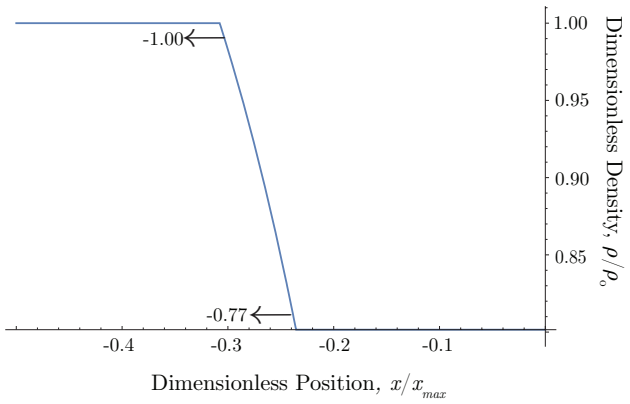

Fig. 3 Rarefaction fan traveling to the left, fundamental derivative $\mathcal{G} > 0$; arrows indicate the direction the wave travels, accompanying numbers indicate the wave speed, normalized by its maximum value on the wave. The leading edge of the fan travels faster than the trailing edge, and the fan continues to spread as it travels.

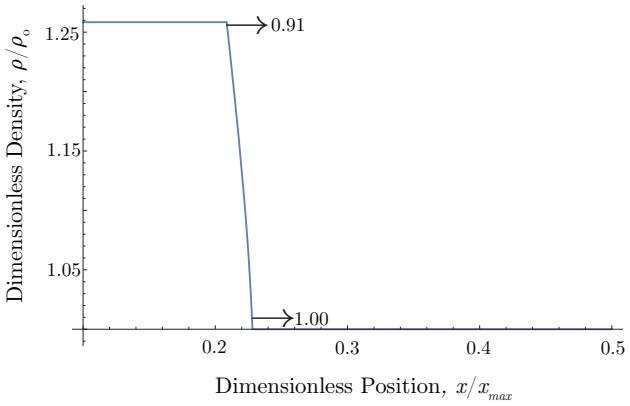

Fig. 4 Compression fan traveling to the right, fundamental derivative $\mathcal{G} < 0$;arrows indicate the direction the wave travels, accompanying numbers indicate the wave speed, normalized by its maximum value on the wave. The leading edge of the fan travels faster than the trailing edge, and the fan continues to spread as it travels, rather than collapsing into a discontinuity.

Anomalous waves may also be observed through the Sod shock tube problem, where one or both of the initial states can be placed within the anomalous region. When both initial states have $\mathcal{G} > 0$, the familiar rarefaction fan, contact discontinuity, and discontinuous compression shock are observed, as in Fig. (6. When both initial states have $\mathcal{G} < 0$, the shock tube instead develops a discontinuous rarefaction shock, a contact discontinuity, and a continuous compression fan, as in Fig. (7.

V. Numerical Method

To solve detonation problems, a numerical scheme is used to solve the governing equations with a piston moving into an ambient fluid. The numerical method that has been chosen is a third order Runge-Kutta method in time and a fifth order weighted essentially non-oscilliatory scheme with mapped weights in space, henceforth referred to as WENO5M; full details are given in Henrick, *et al.* [21]. The WENO5M method is summarized in one dimension with uniform grid spacing, where nodes $j = 0, 1, \ldots, N_x$ have positions x_j, the flux values are given by f_j, and half indices are denoted by subscripts of $i \pm 1/2$. The final form is given by

$$\left.\frac{df}{dx}\right|_{x=x_j} \approx \frac{\hat{f}_{j+1/2} - \hat{f}_{j-1/2}}{\Delta x}, \tag{26}$$

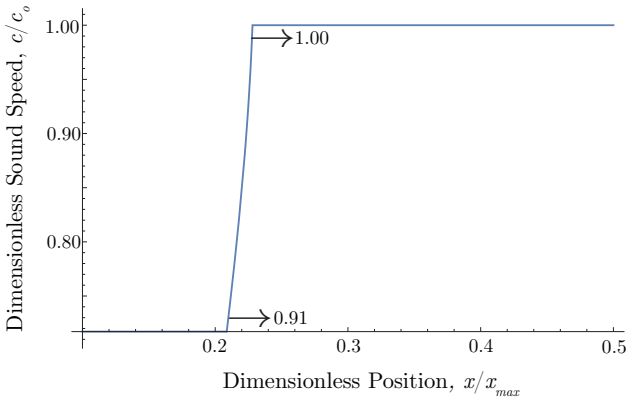

Fig. 5 Change in sound speed across a compression fan with the fundamental derivative $\mathcal{G} < 0$; arrows indicate the direction the wave travels, accompanying numbers indicate the wave speed, normalized by its maximum value on the wave. Although the density increases across the compression, the sound speed decreases.

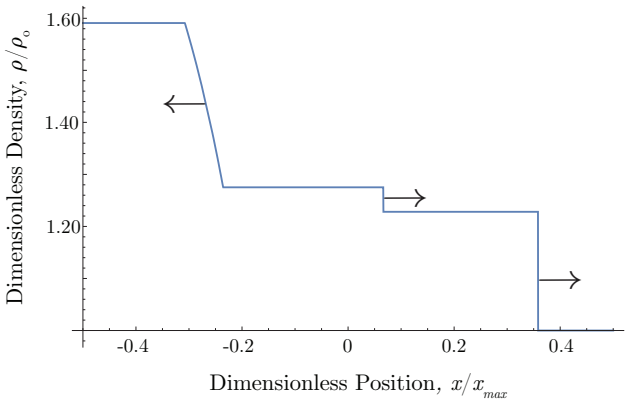

Fig. 6 Shock tube with both initial states having $\mathcal{G} > 0$, arrows indicate the direction each wave travels. The resulting solution is comprised of a left traveling rarefaction fan, a contact discontinuity, and a right traveling compression shock.

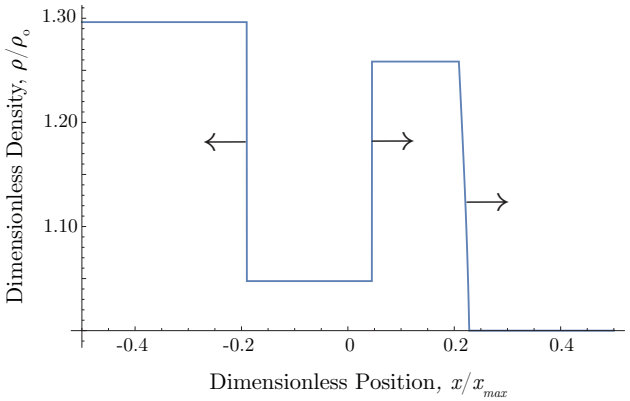

Fig. 7 Shock tube with both initial states having $\mathcal{G} < 0$, arrows indicate the direction each wave travels. The resulting solution is comprised of a left traveling rarefaction shock, a contact discontinuity, and a right traveling continuous compression fan.

where

$$\hat{f}_{j\pm1/2} = \sum_{k=0}^{2} \omega_k^{(M)} \hat{f}^k_{j\pm1/2}. \tag{27}$$

where $\omega_k^{(M)}$ are the mapped weights of the kth stencil, with WENO5M using three stencils $k = [0, 1, 2]$.

The WENO5M scheme as it has been described forces information to propagate from left to right, as a result of the stencil bias. The scheme can be reversed to propagate information from right to left, and is thus constructed by reflecting indices across the $(j + 1/2)$ interface:

$$\hat{h}[f]_{j+1/2} = \begin{cases} \mathcal{F}(f_{j-2}, f_{j-1}, \ldots, f_{j+2}) \\ \mathcal{F}(f_{j+3}, f_{j+2}, \ldots, f_{j-1}). \end{cases} \tag{28}$$

where $\mathcal{F}$ represents the functional form of the WENO method, Eq. (27) for WENO5M. However, we require a scheme that allows for propagation of information in both directions, left to right and right to left. To achieve this, a flux splitting scheme is necessary, as the split fluxes allow the information propagating to the left and the right to be accounted for; the scheme that has been chosen is a global Lax-Friedrichs flux splitting scheme.

VI. Reactions in Non-Ideal Gases

Using the previously described numerical method, along with the parameters and nondimensionalization set by Henrick, *et al.* [22], first an ideal gas solution to the governing equations was produced. Then, a set of values for the van der Waals parameters, a and b, were selected in order to assess their effect on the solutions. These values were chosen to be arbitrary, nondimensionalized values of the van der Waals parameters in order to determine how the non-idealities affect the reaction. Initial runs were done with values that keep the fundamental derivative positive, so a conventional compression shock is produced by a piston. Figure (8) shows the pressure profile behind the compression shock, first with an ideal gas equation of state 8(a), and then with a van der Waals equation of state 8(b), where parameters were chosen to be $a = 1$ and $b = 0.001$. The differences between the ideal gas and van der Waals solutions are not

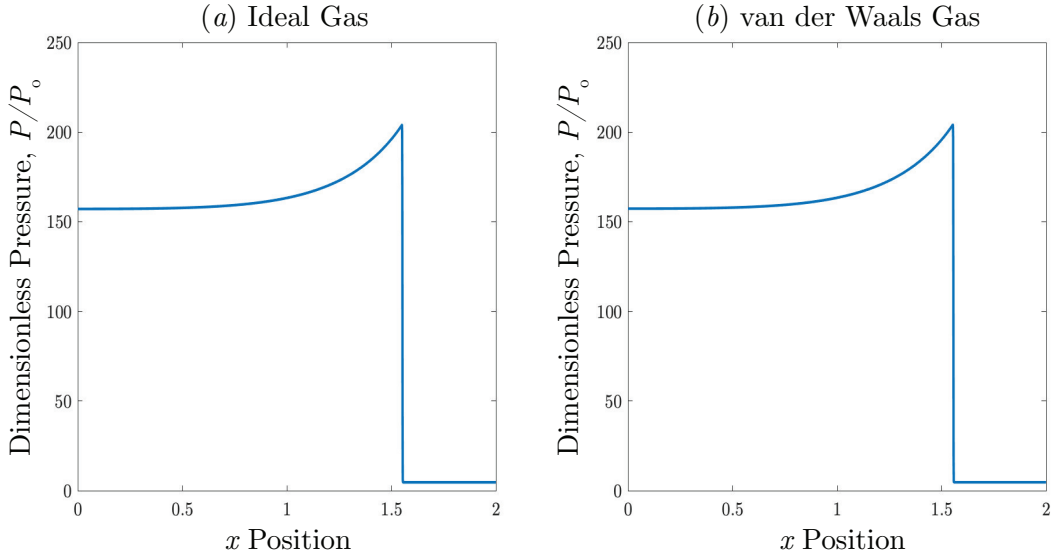

Fig. 8 Pressure behind a shock with reaction. An ideal gas solution is given on the left, and a van der Waals solution, with a = 1 and b = 0.001, is given on the right. Differences are not immediately recognizable here, and the solution seems largely unchanged.

immediately obvious just from the pressure profiles.

Looking instead to the reaction progress, the ideal gas solution was subtracted from the van der Waals solution, and both a and b were varied. The results are shown in Fig. 9. First, b was held at 0.001, while values of $a = [1, 10, 100]$

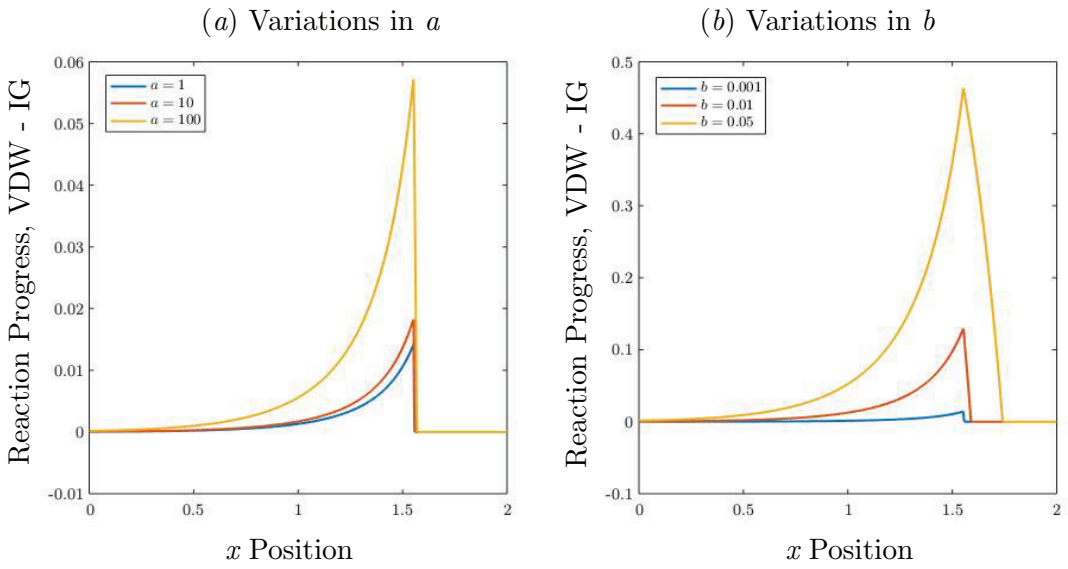

Fig. 9 Reaction progress, ideal gas solution subtracted from the van der Waals solution. In (a), the value of the van der Waals parameter a was varied; small increases in the resulting wave speed were observed, indicated by the "jumps" in the difference. In (b), the value of the van der Waals parameter b was varied; larger increases in the resulting wave speed, as well as the reaction rate, were observed.

were used. As a was increased, the wave in van der Waals solution travels faster than in the ideal gas solution, resulting in the apparent "jump" in the difference. Holding a at 1, values of $b = [0.001, 0.01, 0.05]$ were used. Different values in b resulted in much larger increases in the wave speed, evident by the significant increase in reaction progress as x increases. We look now to the reaction rate itself as the van der Waals parameters a and b are varied, shown in Fig. 10. The difference between the reaction rate at $\lambda = 0.5$ predicted by the ideal gas equation of state was subtracted from

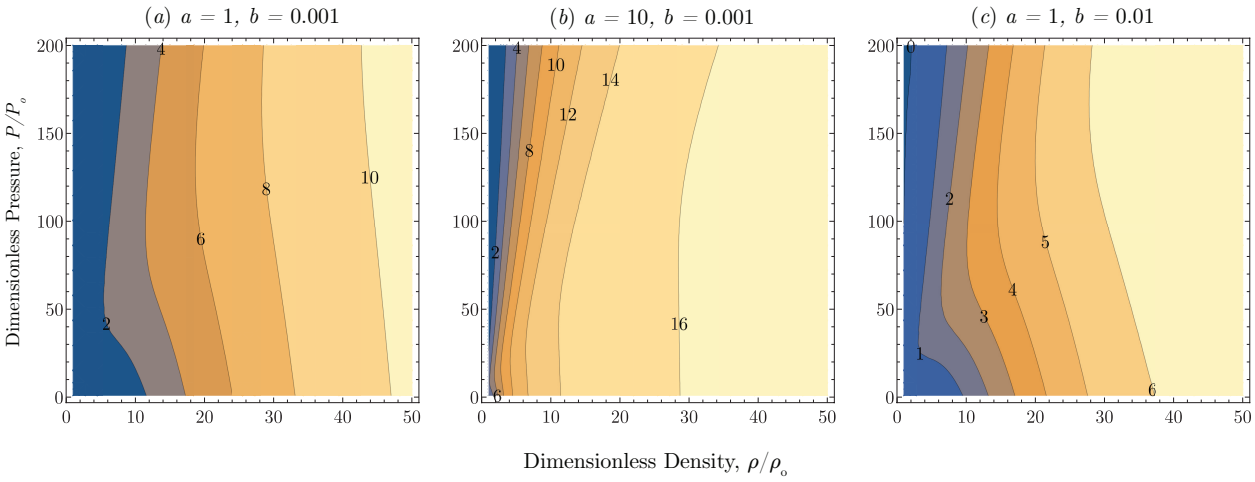

Fig. 10 Reaction rate at $\lambda = 0.5$, ideal gas rate subtracted from van der Waals rate. (a) is the base case of a = 1, b = 0.001, and differences in the reaction rate vary primarily with density. In (b) the value of a has been increased to 10; the reaction rate still differs primarily with density, but varies more quickly with increasing density than for a = 1. For (c), the value of b has been changed to 0.01; this actually results in a decrease in the difference between the ideal and van der Waals rates, varying more slowly with increasing density.

that predicted by the van der Waals equation of state. First, Fig. 10(a) is the base case of $a = 1$, $b = 0.001$, and shows differences in the reaction rate vary primarily with density. In Fig 10(b) the value of a has been increased to 10; the

reaction rate still differs primarily with density, but varies more quickly with increasing density than for $a = 1$. Looking back to Fig. 9(a), this coincides with the increased magnitude of the reaction progress difference as the value of a is increased, even though the compression wave has not traveled significantly faster. For Fig. 10(c), the value of b has been changed to 0.01; this actually results in a slight decrease in the difference between the ideal and van der Waals rates, varying more slowly with increasing density. As a result, the differences seen in Fig. 9(b) can be primarily attributed to the increased speed of the wave.

VII. Conclusions

We have discussed a number of differences in the reaction behind a piston driven compression shock, resulting from changes in both van der Waals parameters a and b. Comparing the ideal gas and van der Waals solutions, obtained with the numerical method described in Section V, it is shown that the non-idealities accounted for by the van der Waals equation of state affect the solution. The parameter a, providing a correction for the intermolecular forces, has a greater effect on increasing the reaction rate as the density increases with respect to the reaction rate for an ideal gas. Changing the value of a has little effect on the speed at which the wave moves through the gas. However, the parameter b, adjusting for the volume occupied by a gas molecule, contributes to much larger increases in the wave speed, as shown in Fig. 9(b). Understanding these changes in the reaction, and how they are brought about by non-ideal parameters of the van der Waals equation, is a key step towards predicting a piston driven detonation into an ambient state where the fundamental derivative $\mathcal{G}$ is less than zero. Starting from the model fluid used by Henrick, *et al.* [22], adjustments must then be made to achieve the desired region of nonconvexity to simulate detonations behind continuous compression fans and split compression waves. The tuning of these parameters is very particular, given the limited nature of regions where $\mathcal{G} < 0$, but will allow for a comparison of reaction properties and detonation stability between the ideal gas model and anomalous waves in the van der Waals model in future work.

Acknowledgments

This study has been supported by Los Alamos National Laboratory, subcontract number 440310. The authors recognize helpful discussions with contract monitor, Dr. Tariq D. Aslam, along with University of Notre Dame undergraduate research student Mr. Alexander M. Davies.

References

[1] Fickett, W., and Davis, W. C., *Detonation*, 1st ed., University of California Press, Berkeley, CA, 1979.

[2] Bethe, H. A., "The Theory of Shock Waves for an Arbitrary Equation of State," Technical Report No. 545, Office of Scientific Research and Development, Washington, DC, 1942.

[3] Zel'dovich, Y. B., "On the Possibility of Rarefaction Shock Waves," *Zhurnal Eksperimental'noi i Teoreticheskoi Fiziki*, Vol. 16, No. 4, 1946, pp. 363, 364. https://doi.org/10.2514/3.13046.

[4] Thompson, P. A., "A Fundamental Derivative in Gasdynamics," *Physics of Fluids*, Vol. 14, 1972, pp. 1843–1849. https://doi.org/10.1063/1.1693693.

[5] Cramer, M. S., "Negative Nonlinearity in Selected Fluorocarbons," *Physics of Fluids*, Vol. 1, No. 11, 1989, pp. 1894–1897. https://doi.org/10.1063/1.857514.

[6] Fergason, S. H., Ho, T. L., Argrow, B. M., and Emmanuel, G., "Theory for Producing a Single-Phase Rarefaction Shock Wave in a Shock Tube," *Journal of Fluid Mechanics*, Vol. 445, 2001, pp. 37–54. https://doi.org/10.1017/S0022112001005444.

[7] Fergason, S. H., Guardone, A., and Argrow, B. M., "Construction and Validation of a Dense Gas Shock Tube," *Journal of Thermophysics and Heat Transfer*, Vol. 17, 2003, pp. 326–330. https://doi.org/10.2514/3.13046.

[8] Colonna, P., and Silva, P., "Dense Gas Thermodynamic Properties of Single and Multicomponent Fluids for Fluid Dynamics Simulations," *Journal of Fluids Engineering*, Vol. 123, No. 3, 2003, pp. 414–427. https://doi.org/10.1115/1.1567306.

[9] Colonna, P., and Rebay, S., "Numerical Simulation of Dense Gas Flows on Unstructured Grids With an Implicit High Resolution Upwind Euler Solver," *Journal of Numerical Methods, Fluids*, Vol. 46, No. 7, 2004, pp. 735–765. https://doi.org/10.1002/fld.762.

[10] Colonna, P., and Guardone, A., "Siloxanes: A New Class of Candidate Bethe-Zel'dovich-Thompson Fluids," *Physics of Fluids*, Vol. 19, No. 8, 2007. https://doi.org/10.1063/1.2759533.

[11] Colonna, P., and Guardone, A., "Molecular Interpretation of Nonclassical Gas Dynamics of Dense Vapors Under the van der Waals Model," *Physics of Fluids*, Vol. 18, No. 5, 2006. https://doi.org/10.1063/1.2196095.

[12] Harink, J., Guardone, A., and Colonna, P., "The Influence of Molecular Complexity on Expanding Flows of Ideal and Dense Gases," *Physics of Fluids*, Vol. 21, No. 8, 2009. https://doi.org/10.1063/1.3194308.

[13] Cramer, M. S., and Sen, R., "Shock Formation in Fluids Having Embedded Regions of Negative Nonlinearity," *Physics of Fluids*, Vol. 29, No. 7, 1986, pp. 2181–2191. https://doi.org/10.1063/1.865555.

[14] Cramer, M. S., and Crikenberger, A. B., "The Dissipative Structure of Shock Waves in Dense Gases," *Journal of Fluid Mechanics*, Vol. 223, No. 1, 1991, pp. 325–355. https://doi.org/10.1017/S0022112091001441.

[15] Cramer, M. S., "Shock Splitting in Single-Phase Gases," *Journal of Fluid Mechanics*, Vol. 199, 1989, pp. 281–296. https://doi.org/10.1017/S0022112089000388.

[16] Guardone, A., Zamfirescu, C., and Colonna, P., "Maximum Intensity of Rarefaction Shock Waves for Dense Gases," *Journal of Fluid Mechanics*, Vol. 642, 2007, pp. 127–146. https://doi.org/10.1017/S0022112009991716.

[17] Zamfirescu, C., Guardone, A., and Colonna, P., "Admissibility Region for Rarefaction Shock Waves in Dense Gases," *Journal of Fluid Mechanics*, Vol. 559, 2008, pp. 363–381. https://doi.org/10.1017/S0022112008000207.

[18] Menikoff, R., and Plohr, B. J., "The Riemann Problem for Fluid Flow of Real Materials," *Review of Modern Physics*, Vol. 61, No. 1, 1989, pp. 73–130. https://doi.org/10.1103/REVMODPHYS.61.75.

[19] von Mises, R., *Mathematial Theory of Compressible Fluid Flow*, Academic Press, New York, 1958.

[20] Courant, R., and Friedrichs, K. O., *Supersonic Flow and Shock Waves*, Interscience Publishers, New York, 1948.

[21] Henrick, A. K., Aslam, T. D., and Powers, J. M., "Mapped Weighted Essentially Non-Oscillatory Schemes: Achieving Optimal Order Near Critical Points," *Journal of Computational Physics*, Vol. 207, No. 2, 2005, pp. 542–567. https://doi.org/10.1016/j.jcp.2005.01.023.

[22] Henrick, A. K., Alsam, T. D., and Powers, J. M., "Simulations of Pulsating One-Dimensional Detonations with True Fifth Order Accuracy," *Journal of Computational Physics*, Vol. 213, No. 1, 2006, pp. 311–329. https://doi.org/10.1016/j.jcp.2005.08.013.